energies

MDPI

Review

Research Progress on Thermal Hydraulic Characteristics of Spent Fuel Pools: A Review

Chende Xu [1], Zhengguang Wang [1], Shuai Tang [2], Xiangyu Chi [2], Xixi Zhu [2], Yaru Li [2] and Naihua Wang [2,*]

[1] State Key Laboratory of Nuclear Power Safety Monitoring Technology and Equipment, China Nuclear Power Engineering Co., Ltd., Shenzhen 518031, China
[2] Institute of Thermal Science and Technology, Shandong University, Jinan 250022, China
* Correspondence: wnh@sdu.edu.cn

Abstract: Nuclear power plants (NPPs) produce large amounts of spent fuel while generating electricity. After the spent fuel is taken out of the reactor core, it still has a high decay heat and needs to be cooled for years or even decades before it can be reprocessed or buried deeply. Due to the long storage period of spent fuel, storage safety evaluation is a concern. In this regard, cooling systems are critical for the safe storage of spent fuel. Here, the research progress of cooling methods for spent fuel pools (SFPs) is reviewed, and the structural characteristics, application limitations and heat transfer performance of active and passive cooling technologies under accident conditions are discussed in detail. Moreover, future developments of SFPs are discussed, and the results of this review confirm that there is a great deal of research scope to improve the cooling performance and safety of spent fuel. This paper aims to provide a reference guide for engineers and will be highly beneficial to researchers engaged in spent fuel storage.

Keywords: spent fuel pool; thermal hydraulic characteristics; loss-of-coolant accident; passive cooling system

Citation: Xu, C.; Wang, Z.; Tang, S.; Chi, X.; Zhu, X.; Li, Y.; Wang, N. Research Progress on Thermal Hydraulic Characteristics of Spent Fuel Pools: A Review. *Energies* **2023**, *16*, 3990. https://doi.org/10.3390/en16103990

Academic Editor: Mahmoud Bourouis

Received: 17 April 2023
Revised: 3 May 2023
Accepted: 8 May 2023
Published: 9 May 2023

1. Introduction

As an economical and efficient low-carbon energy source, the use of nuclear power has reduced carbon dioxide emissions by approximately about 70 billion tons in the past half century [1,2]. In 2021, 9.84% of global electricity was generated by nuclear energy, which plays an irreplaceable role in helping countries achieve carbon neutrality [3]. However, as the installed capacity of NPPs has increased, the amount of spent fuel has also increased year on year, and the storage of spent fuel has become an important problem restricting the development of nuclear power in various countries. Spent fuel is the fuel unloaded from the reactor after combustion, which contains high levels of radionuclides and releases a large amount of decay heat, with a high recovery value [4]. Some countries have explicitly adopted closed-cycle nuclear fuel policies, but there is still a large gap between the annual spent fuel disposal capacity and output [5,6], and intermediate storage is a necessary means through which to mitigate the rising amount of spent fuel.

Generally speaking, after the spent fuel is removed from the reactor, it will be stored in an SFP for several years or even decades. The SFP provides (a) shielding from radiation generated by spent fuel decay and (b) cooling of the heat generated by spent fuel decay. Nowadays, more than 400 NPPs have built SFPs around the world. However, following the 2011 Fukushima nuclear accident in Japan, researchers realized the possibility of the serious failure of SFP cooling systems [7,8] and this accident led to the introduction of greater requirements for the way spent fuel is cooled.

The safety of spent fuel has always been a hotspot for scholars. Moamen et al. [9] re-viewed the design and development of dry storage barrels; Laura [10] et al. summarized the mode and management technology of the spent fuel cycle; Zhang et al. [11]

commented on the differences in health and safety culture among different positions in an NPP; Saegusa et al. [12] investigated the transport and storage of spent fuel; Hu et al. [13] reviewed the research progress in the treatment of spent fuel via machine learning; and Surip et al. [14] systematically reviewed the heat transfer characteristics of two-phase heat pipes in passive heat transfer systems. Many experts have carried out research on the policy, design, extraction, transportation and utilization of spent fuel, but the existing literature shows that there are few reviews on the thermal hydraulic characteristics of SFPs, with minimal discussions around cooling methods. Therefore, this paper reviews the thermal hydraulic development of SFPs in recent years and the main objectives of the review are as follows:

The review mainly focuses on the thermal hydraulic characteristics of SFPs under normal cooling conditions and accident conditions. Section 2 of this paper reviews the cooling systems of SFPs, Section 3 comments on the research reports in the event of an SFP accident, while Section 4 comments further on the research results of this paper and puts forward the development directions for SFP cooling technology in the future.

2. SFP Cooling System

According to the different driving forces of the cycle, SFP cooling systems can be divided into active and passive modes. Active cooling systems consume electric energy to maintain operation, while passive cooling systems (PCSs) do not consume energy. Active cooling systems circulate and cool pool water under the action of a pump and an external heat exchanger (Figure 1a). Passive cooling systems depend on natural convection, diffusion, evaporation, condensation, height differences and other natural laws to achieve operation (Figure 1b). This section describes in detail previous studies of active cooling systems and PCS in terms of system configuration, experimental design and numerical simulation.

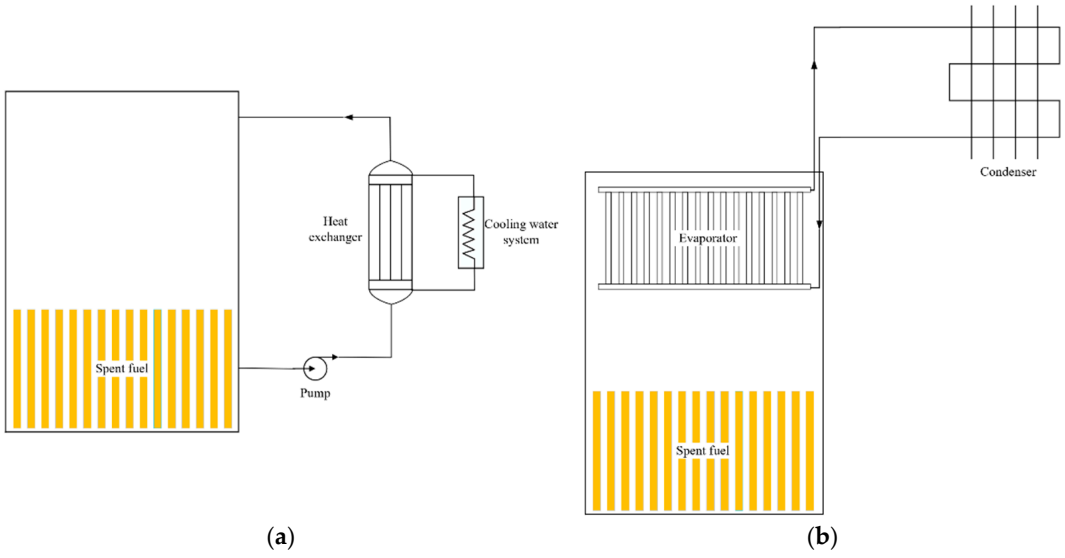

Figure 1. SFP cooling system. (**a**) Active cooling system. (**b**) Passive cooling system.

2.1. Scheme of SFP Cooling System

At present, the main cooling mode of SFPs is active circulation, which mainly consists of five parts: a water pool, a loop, a circulating pump, a heat exchanger and a filter. The loop system consists of four loops: cooling, purification, filling and draining. Driven by the pump, the water temperature is kept below 50 °C [15]. With the development of nuclear power technology, the cooling schemes of SFPs present a variety of characteristics. Table 1 compares the configurations of five main reactor-type spent fuel cooling systems.

Table 1. Configuration comparison.

Reactor Type	Safety-Level Loop/Column	Pump/Set	Heat Exchanger/Set	Extra Cold Source
M310 [16]	2	2	2	No
EPR [17]	3	5	3	Yes
VVER [18]	2	2	2	No
AP1000 [19,20]	2	2	2	Yes
HPR1000 [21]	3	3	3	Yes

It can be seen from Table 1 that the Generation-II reactor represented by M310 is equipped with two safety-level cooling systems for the SFP. Each column consists of a heat exchanger and a horizontal centrifugal pump. Considering the unloading of the unit and the maintenance of the electrical or cooling system of one column, only one cooling circuit remains in the cooling system. Both the supply of water and the cooling of the PTR system are operated by pumps. Once station blackout (SBO) or feedwater line break (FLB) occurs, the SFP cannot be continuously cooled, and the reaction time required to prevent an accident will be extremely short.

The Generation-II reactor represented by EPR is equipped with three rows of safety-level cooling systems for the SFP. Compared with M310, the system's redundancy is increased, in which two main columns are equipped with double pumps and a standby power supply scheme is adopted in a power supply setting. The cold source of the heat exchanger is also considered in relation to redundancy. In addition, the third column is equipped with a diversified water cooling system. Although the redundant design improves the safety factor, it also increases construction costs.

VVER originated from the Generation-III reactor of the Soviet Union, and it is equipped with two safety-level SFP cooling systems. The design concept is similar to that of the first two reactor types, but the difference is that the SFP and refueling pool are integrated and arranged within the containment.

AP1000 is an advanced passive pressurized water reactor nuclear power technology. The most important feature of AP1000 is its concise design, easy operation and full utilization of many "passive safety systems" [20]. In the system design, two rows of non-safe cooling systems are arranged for the SFP. In the event of SBO accidents, the safe passive containment cooling system's water storage tank can be used as supplementary cold water source, which can realize the passive cooling of the SFP within 3 days.

HPR1000 adopts three safety-level cooling loops, which consider the re-supply design from different power sources during unit maintenance and add an additional cooling system to the heat exchanger as a redundant cooling source, further increasing the reliability of the spent pool cooling function. In addition, HPR1000 employs effective passive safety measures based on active safety and is equipped with a passive water supply system [22].

From this comparison of five cooling system schemes, in order to improve safety, NPPs are continuing to expand the principle of redundancy. As a result, although the probability of accidents has decreased, systems have become increasingly complex, and the investment and construction period of nuclear energy have obviously increased. To some extent, safety depends on the external energy drive system: once a problem occurs within a spent fuel energy supply system, it may have serious consequences, and this safety problem has not yet been solved. It has been suggested that air cooling could increase diversified heat dissipation methods and, at the same time, increase the water supply interface, making it more convenient for mobile devices to connect. Regarding passive cooling methods, the passive design of SFPs is only in the initial stages. The water loss time of the SFP in Fukushima nuclear power plant far exceeds the preset 72 h of AP1000 and its passive cooling capacity is very limited, which shows that the passive cooling capacity of the existing reactor needs to be enhanced.

2.2. PCS of SFP

The Fukushima nuclear accident has been recognized by IAEA as a level 7 safety accident, and all countries are actively seeking and designing methods to improve the safety of NPPs. According to the design requirements of the IAEA safety standards, NPPs should control the development of accidents through passive safety systems or other systems that can still operate continuously [23]. Passive safety systems depend on natural convection, diffusion, evaporation, condensation and other natural laws such as height differences and compressed gases and fluids to achieve operation. They do not require a power supply in the form of a pump, an AC power supply, an engine generator, etc. The introduction of the concept of passive safety reduces the redundancy of the system, improves the human–machine relationship, enhances the safety, reduces the construction cost and fundamentally changes the design of NPP safety systems [24]. The temperature of SFPs is between 30 and 90 °C, and the temperature of heat sink is between 20 and 40 °C. In the event of SBO, the decay heat that needs to be released can reach 16 MW in extreme cases. In view of the problems of small temperature differences and large heat transfer, loop heat pipe technology has attracted wide attention. Heat pipes are widely used in the PCSs of large equipment [25–27].

2.2.1. Design Scheme of PCS

Westinghouse Corporation designed a floating PCS for an SFP [20]. A gravity heat pipe module is arranged at the upper end of the SFP and when the power is lost, the heat pipe is used for cooling. According to its design scheme, each heat pipe can take away 300 kW of heat, which can ensure that the temperature of the SFP remains below 60 °C. As an independent standby system, it can be used to passively cool the pool and cooperate with the replenishing water system to ensure water level safety. Although the system can effectively take away the decay heat of spent fuel, it also has some disadvantages, such as the large floor space required and the fact that the sight of the pool is blocked.

In 2012, AREVA Corporation proposed a single-phase heat pipe to derive heat from SFP [28]. The system consists of a water–water heat exchanger, a water–air heat exchanger, a loop heat pipe and a fan. The water–water heat exchanger is fixed above the spent fuel tank, while the water–air heat exchanger is arranged in the cooling tower outside the powerhouse of the SFP. The fan is arranged in the air-cooling tower to enhance convection heat exchange. The fan requires energy to operate, which is inconsistent with the non-energy design concept. However, cooling the SFP with separate heat pipes is a potential development direction.

In order to improve the heat exchange capacity of PCS, there are two main methods: (1) reduce the thermal resistance of the heat exchanger; (2) reduce the flow resistance of the working medium. Based on the two methods, AREVA continues to develop a two-phase PCS. The system consists of a condenser, an evaporator and a loop heat pipe. The working medium boils in the evaporator, taking away the heat in the fuel pool. The density difference between the ascending tube (gas) and the descending tube (liquid) is large enough to overcome the additional flow resistance introduced by two-phase flow, and the liquid temperature difference between the ascending channel and the descending channel is small. When the maximum temperature difference is constant, the heat transfer driving force is greater, and a condenser with a smaller heat exchange area can discharge the same amount of heat as a single-phase cooling system, which enhances the heat exchange capacity of the system and reduces the construction cost.

Fujikura Company put forward a cooling scheme for an SFP based on a loop heat pipe [29,30], which is a completely passive system and can work normally under harsh conditions. The evaporator is arranged next to the spent fuel tank and the condenser is located outside the plant, while the heat exchange capacity can reach 4 MW. Mukhsinun et al. [31–33] built a vertical straight wickless-heat pipe PCS test bench, where the maximum power is 2500 W and the heat trap is water (see Figure 2). Choi et al. [34,35] proposed a passive spent pool cooling system using a fork-end heat pipe (see Figure 3). The system mainly

consists of three parts: a condenser composed of 12 tubes with round fins, an adiabatic header and a single-tube evaporator. The heat transfer capacity is 2.1 kW.

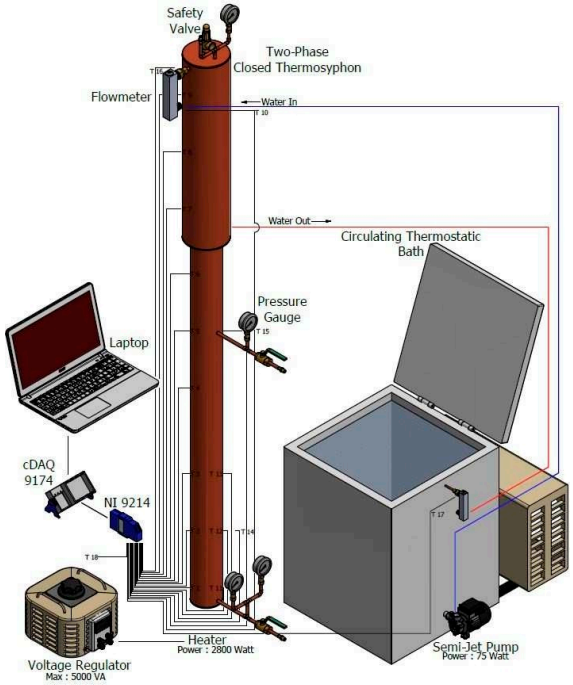

Figure 2. PCS of a straight wickless-heat pipe [31].

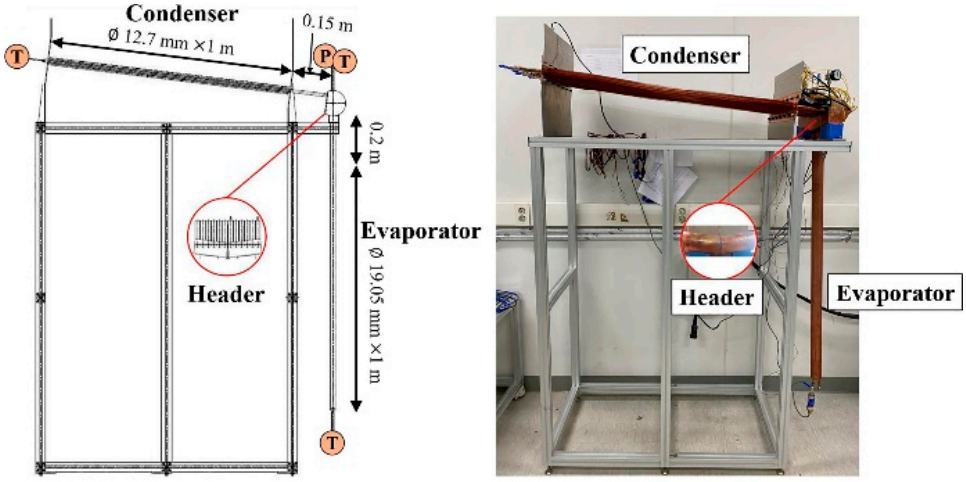

Figure 3. PCS of a fork-end heat pipe [34].

Based on CAP1400 SFP, Ye et al. [36,37] designed and simulated a PCS, and Xiong [38–40] et al. established a large-scale separated single heat pipe system for experimental verification, as shown in Figure 4. The experimental evaporation section is 7.6 m, the diameter is 76 mm, the condensing section is 20 m long, and it is formed by winding stainless steel finned tubes in a snake shape. The results show that the system has a strong heat transfer capacity with the maximum heat transfer capacity reaching 20.1 kW. Zheng et al. [41] developed a coupled interface with MELCOR and RELAP to simulate the transient heat transfer process of a passive cooling system. Li and Kuang [42,43] proposed a separate heat pipe with a built-in tube system. Many researchers have designed PCSs and achieved varying results. Table 2 summarizes the main features of a PCS. It can be concluded that the research on the passive cooling of spent fuel pools mainly focuses on separated heat pipes, and the cold sources utilized can be divided into air and water. The overall research is mainly based on experiments.

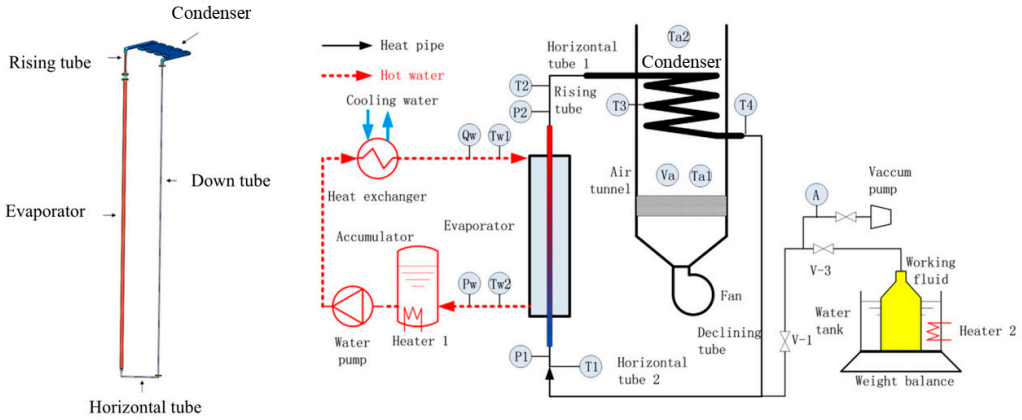

Figure 4. PCS of a large-scale separated single heat pipe [38].

Table 2. The main features of the PCS.

	Author	Type	Research Method	Final Heat Sink	Maximum Heat Transfer Capacity
1	Westinghouse [20]	Gravity heat pipe	Experiment	Atmosphere	300 kW (single heat pipe)
2	AREVA [28]	Heat pipe loop	Experiment	Atmosphere (air cooling tower)	1.25 MW
3	Fujikura [29]	Heat pipe loop	Experiment	Atmosphere	4 MW
4	Kusuma [31]	Straight wickless-heat pipe	Experiment	Water	2.5 kW
5	Choi [34]	Fork-end heat pipe	Experiment	Atmosphere (air cooling tower)	2.1 kW
6	Ye [36]	Heat pipe loop	Simulation (Fluent)	Atmosphere	16 MW
7	Xiong [38]	Large-scale separated single heat pipe	Experiment	Atmosphere (air cooling tower)	16.8 kW
8	Zheng [41]	Heat pipe loop	Simulation (MELCOR and RELAP5)	Atmosphere	-
9	Li [42]	Shell-and-tube heat exchanger	Simulation (RELAP5)	Atmosphere	11.98 MW
10	Kuang [43]	Large-scale separated single heat pipe	Simulation; experiment	Atmosphere	-
11	Wu [44]	Separated heat pipe with compact structure	Experiment	Atmosphere	4 kW
12	Luo [45]	Multi-parallel branch-separated heat pipe	Experiment	Water	-

2.2.2. Research on Heat Transfer Capacity of PCS

To improve the passive cooling capacity, researchers are committed to studying different factors affecting the heat transfer performance of passive cooling systems, such as equipment layout, equipment shape, working fluid, filling rate, temperature, cooling wind speed, etc.

The natural convection of pool water is a sufficient condition for the operation of a PCS. The process of natural circulation in an SFP can be subdivided into three stages: in the first stage, the temperature of the pool water gradually produces thermal plumes; in the second stage, the formation of thermal stratification occurs; and in the third stage, a steady state of natural convection circulation is reached. Han et al. [46] designed two layouts to study the effect of the heat exchanger arrangement on the flow pattern in an SFP, as shown in Figure 5. It is suggested that the proper distance between the heat exchanger and the wall is conducive to the formation of natural convection.

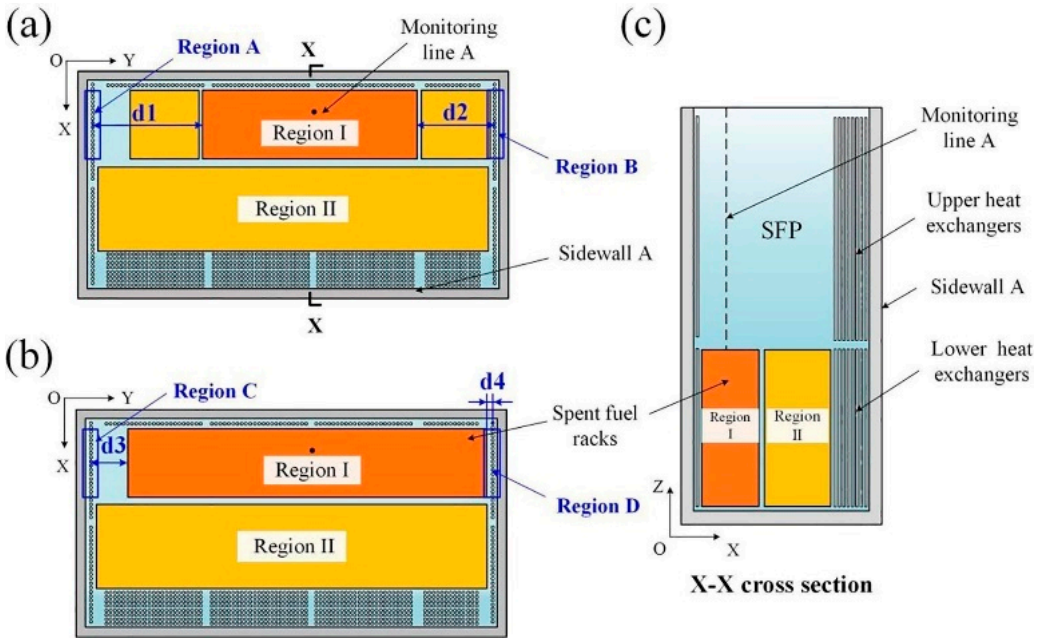

Figure 5. Layout of an SFP by Han et al. [46]. (**a**) top view of Layout A, (**b**) top view of Layout B, and (**c**) X-X cross-section.

Xiong et al. [38–40] selected water, R134a and ammonia as working fluids to conduct a separate monomer heat pipe experiment. The operating conditions were as follows: the flow rate of the heat source was 0.7–2.1 $\times$ 10^{-2} m/s, the heat source temperature was 50–90 °C and the speed of cooling air was 0.5–2.5 m/s. The results show that these three working fluids can be used for PCS, the heat transfer performance of ammonia is better and the heat source temperature has a great influence on the heat transfer performance of the heat pipe. Based on the experiments of Xiong et al. [40], Kuang et al. [47] established a mathematical model of a large separated heat pipe (as shown in Figure 6) and used ammonia, R134a and water as working fluids to study their effect on the long-distance heat transfer capacity of heat pipes. The results show that the pressure loss of the water heat pipes is the largest. Ammonia and R134a working fluids are more suitable for long-distance heat transfer. Compared with water and R134a heat pipes, ammonia heat pipes have the best heat transfer performance, providing an additional 40% heat transfer capacity [48]. Moreover, Kuang et al. [49] pointed out that the optimal filling rate of a water–heat pipe is about 17%, and the optimal filling rate of an R134a or ammonia heat pipe is between 20% and 70%. An excessive or low filling rate will result in a reduced heat transfer capacity. Fu et al. [50] simulated the experimental results of Xiong et al. [40] and analyzed the flow and heat transfer characteristics of a PCS using RELAP5 code. The thermal hydraulic decoupling analysis methods for natural water circulation in an SFP are shown in Figure 7. The velocity and temperature distribution in the SFP were numerically simulated using Fluent. Fu et al. pointed out that the filling rate of the working medium should be between 30% and 80%. By comparing the above studies, it can be seen that ammonia water has stronger heat transfer characteristics than water and R134a and is more suitable for long-distance transmission. However, ammonia is toxic and has a pungent smell, and the discussion of the chemical properties of the working fluid in the above article is not clear.

Kusuma et al. [32] carried out PCS experiments to validate the RELP5/MOD 3.2 model. The results show that the optimum filling rate is 60%. Graphene nanofluid with a mass concentration of 1% was selected as the working fluid [51]. At a filling rate of 80%, a higher heat load and a higher coolant volume flow rate, a vertical straight coreless heat pipe with graphene nanofluids as the working fluid has a higher thermal performance than a heat pipe filled with demineralized water. Graphene nanofluids can improve the thermal characteristics of loop heat pipes. The optimal working fluid and filling rate of different

heat pipe structures are also different. However, there has not been a comprehensive discussion on the physical phenomena behind the optimal values of nanofluids.

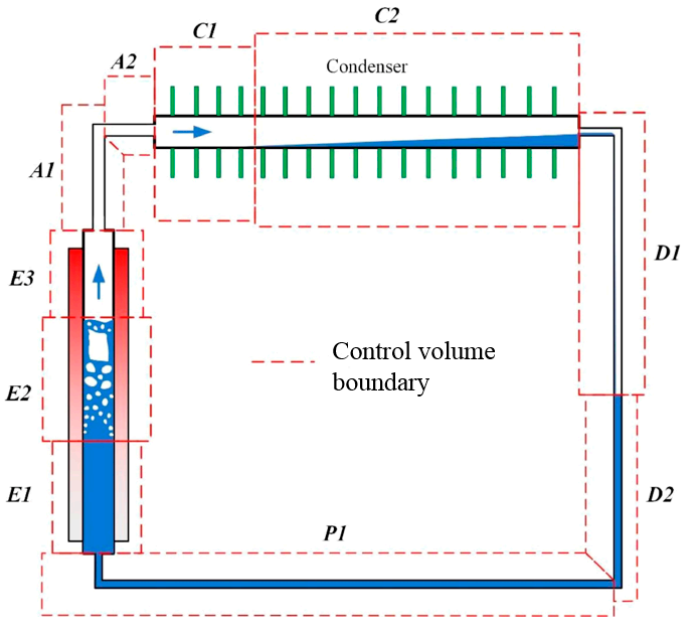

Figure 6. Analysis model [48].

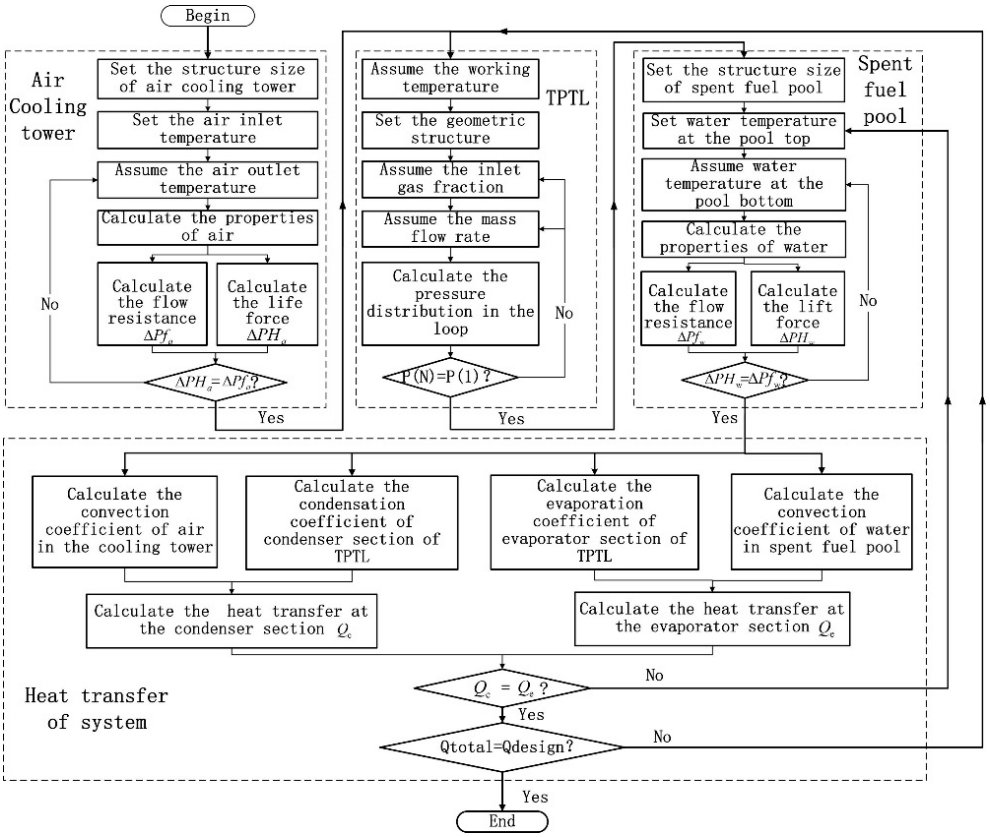

Figure 7. The analysis method for a PCS [50].

To further clarify the working mechanisms of the heat pipe working medium, Lim et al. [35] studied the boiling heat transfer characteristics in the evaporation of a fork-type heat pipe with water as the working fluid (see Figure 8). In the evaporator, nucleate boiling occurs in the upper part of the evaporator as the liquid at the bottom gradually overheats. With the

continuous accumulation of heat, intermittent boiling occurs at the bottom level, resulting in massive flow and annular flow. The bubbles then rise to the outlet in the vertical evaporator tube and rapidly expand. When the bubbles become large enough, the large, blocked bubble flow sweeps the working fluid out of the evaporator. As part of their research on the heat transfer coefficient of working medium evaporation boiling in a heat pipe, Kundu et al. [52] pointed out that the heat transfer coefficient of the working medium increases with the increase in the steam mass flow rate. Under the same mass flow rate, the heat transfer coefficient of the working medium depends on the heat flux before dry-out occurs. Enoki et al. [53] studied the evaporation boiling process of water. They pointed out that the heat transfer process of water not only consists of boiling heat transfer and forced convection heat transfer, but also includes thin liquid film heat transfer. At a low heat flux rate, thin liquid film thermal evaporation dominates. The study of Kuang et al. [54] shows that for ammonia and R134a, due to the low wall heat flux and low surface tension, nucleate boiling is the main heat transfer mechanism. At the condensation end of a passive cooling system, fully stratified flow is the main flow mode. Kuang et al. [49] pointed out that there are two heat transfer mechanisms for the condensation of saturated steam on the inner wall of the tube and the gas–liquid interface: membrane condensation on the tube wall and conduction condensation in the tube. They therefore proposed a condensation model in the tube, which greatly reduces the calculation error. The gas–liquid distribution and boiling intensity of the working medium in the heat pipe are important factors affecting the heat transfer performance of a PCS.

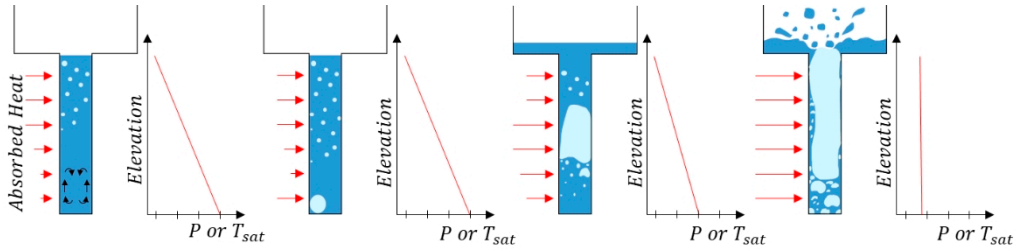

Figure 8. Boiling form in evaporator [35].

Wu et al. [44] studied the effects of inlet air volume, inlet air temperature and the angle of inclination on the heat transfer process. The experimental results show that the heat transfer capacity of the heat pipe is improved in the inclined state, while the optimal temperature at the condensing end is about 30 °C. Lima et al. [55] studied the thermal hydraulic stability of PCS through linear and nonlinear models. The results show that there is no qualitative relationship between the water volume in the pool and the stability of the system. Shandong University [56,57] established a loop heat pipe test bench, studied the heat transfer and resistance characteristics of the passive cooling system of an SFP based on a loop heat pipe, proposed an optimized thermal hydraulic system design method and determined the natural circulation working point, the optimal filling rate and the height difference.

The final heat sink of passive cooling systems generally has three designs. The first is direct air cooling, the second is the use of an air-cooling tower and the third is the use of water-cooling tank. Due to the height difference of the loop, the third type is rarely used. Lai et al. [58] discussed the convection heat transfer of the condenser of a large-scale separated single heat pipe PCS and pointed out that the arrangement of the cooling tower can enhance the flow and heat transfer capacity. The fin spacing, fin height, outlet temperature of the cooling tower and inlet velocity of the cooling air are the key factors affecting the heat transfer performance. The optimal gap of the tube spacing is between 0.2 m and 0.3 m, the optimal range of the fin height is 0.03 m–0.04 m, the optimal range of the cooling tower outlet temperature is 40–45 °C and the optimal air inlet speed is 1.0 m–1.5 m. The intensity of natural air convection is related to buoyancy and viscosity. When buoyancy is greater than viscosity, high-intensity convective heat transfer will occur. Unger et al. [59–61]

simulated the heat transfer characteristics of a finned-tube condenser under natural air convection conditions in a cooling tower (as shown in Figure 9), and determined that the best finned tube structure is a round fin or an elliptical finned tube with an axial ratio of 1:2.1. It is pointed out that when the height of the cooling tower is more than 11 m, it has little effect on the heat transfer capacity. The natural convection heat transfer intensity of the cross arrangement is obviously higher than that of the parallel arrangement. With the decrease in the longitudinal tube spacing, the heat transfer performance is enhanced. The heat transfer effect is optimal when the horizontal spacing is 64 mm in the parallel arrangement and the time spacing of the cross arrangement is 65 mm. The heat transfer effect is not significant when the number of tube rows is greater than five. From the above analysis, it can be seen that PCS can remove residual heat more quickly via the use of cooling towers. However, the parameters of condenser fins are variable under different decay powers. In order to determine the optimal heat transfer conditions of the condensing end of a passive cooling system, attention must be paid to different fin shapes, such as wavy fins, flat fins, serrated fins, etc.

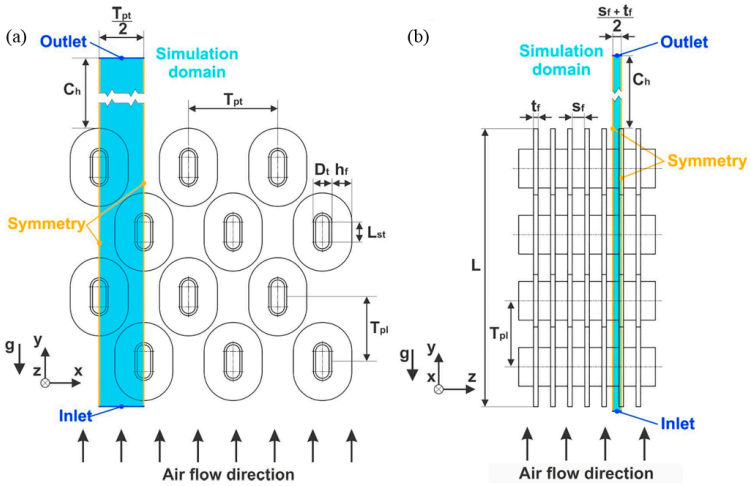

Figure 9. Nomenclature and boundary conditions of heat exchanger and simulation domain [59]. (**a**) front view and (**b**) side view.

In summary, the current study proves that the passive cooling capacity of SFPs is seriously insufficient, and there is a safety risk in the event of SBO. At the same time, the existing research shows that the passive cooling of SFPs can be realized by the use of separated heat pipes, but this is still in the experimental stages, and the theoretical models and experimental data are relatively lacking. There is still a long way to go when it comes to implementing PCSs in practical applications. It is necessary to further explore PCSs to improve our understanding of their thermal hydraulic characteristics.

3. Research on Safety of SFPs

At present, the research on the safety of SFPs mainly focuses on the field of thermal hydraulic analysis. This section reviews the heat transfer process and potential problems in the event of accidents, as well as evaluating the thermal hydraulic analysis programs and emergency mitigation measures in the event of an accident.

3.1. Loss-of-Coolant Accident in SFPs

Spent fuel still has high energy after being discharged. Rigby [62] et al. used exergy as a measure to analyze the sustainability of the nuclear fuel cycle. There is still a large amount of exergy in spent fuel, and most of it is utilized as potential fission exergy loss. Therefore, research into the safety of spent fuel storage is particularly crucial. The heat transfer conditions of SFPs can be divided into three stages: (a) spent fuel completely covered by water; (b) spent fuel partially exposed; and (c) spent fuel completely exposed,

as shown in Figure 10. When the active cooling system of an SFP operates normally, the pool water flows downwards along the channel between the pool wall and the storage racks; then, it flows upward after passing through the base of the storage racks and enters the interior of the fuel assembly. The pool water absorbs the decay heat of the component, increasing the temperature and decreasing the density; then, it flows to the upper part of the rack and is mixed with cold water. After mixing, the temperature of the pool water decreases and the density increases, and the pool water then flows downward along the flow path between the storage rack and the pool wall, creating natural circulation in the pool [63,64], as shown in Figure 10a.

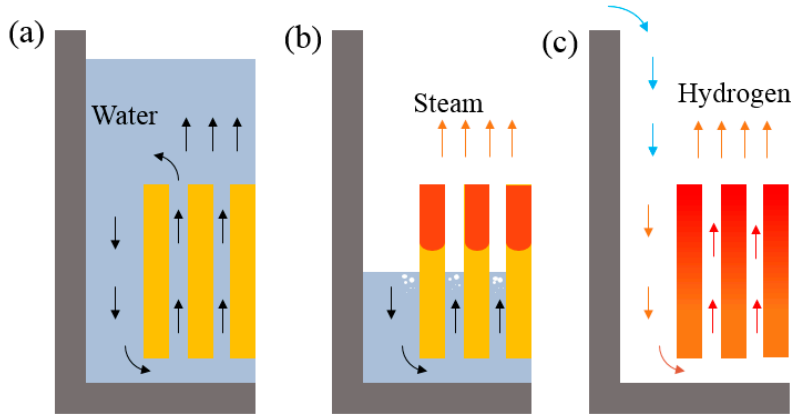

Figure 10. Thermo-hydraulic conditions in three stages of an SFP. (**a**) normal operation (**b**) partially exposed (**c**) completely exposed.

Figure 10b,c displays a loss-of-coolant accident (LOCA). A LOCA can be caused by SFP connection tube leakage, SFP structural integrity damage and cooling system failure or insufficient cooling capacity. When a LOCA occurs, the SFP can only rely on natural circulation to reduce the decay heat of spent fuel. At this time, the temperature of the pool water rises continuously and, after a long enough time, the pool water begins to boil. If this boiling continues, the water level drops, exposing the spent fuel or even exploding, thus causing the release of radioactive materials and posing a serious threat to public and environmental safety.

In 1979, Benjamin et al. [65] studied the thermal hydraulic characteristics of an SFP in the event of a loss-of-water accident. It was found that the heat transfer of the SFP depends on the decay time of the spent fuel, the design structure of the storage rack, the packing density and the ventilation characteristics of the building. At the same time, it was pointed out that the failure of the fuel cladding during the accident is closely related to the storage rack structure and the decay time of the spent fuel. NUREG/CR 5281 [66], issued by the Nuclear Regulatory Commission of the United States, pointed out that in order to reduce the risk to SFPs, the storage density of spent fuel should be reduced and spray facilities, a make-up water system and a backup cooling system should be installed to prevent and mitigate accidents. Jo [67], and Throm [68] point out that the initial temperature of an spent fuel cladding fire is 900 °C, making it a particularly serious fire. However, compared with a reactor core accident, the probability of a spent fuel cladding fire accident is extremely low, so it is not necessary to take any measures to improve existing SFPs [69]. The above report provides technical support for the storage of as much spent fuel as possible within the limited space of an SFP. It is also suggested that the storage racks from a loose array be changed to a dense array. After the 9/11 attack, the NRC required that spent fuel with a high decay heat should be dispersed in the pool instead of concentrated in one place to reduce the risk of an aircraft attack on the reactor and SFP. In particular, in the case of an aircraft attack, backup water for the pool should be provided. However, these measures are insufficient to ensure the security of SFPs in accidents and attacks.

According to the loss of the water level, a LOCA can be divided into a partial loss-of-coolant accident and a total loss-of-coolant accident. The heat transfer process of a partial loss-of-coolant accident in an SFP mainly includes the evaporation/boiling heat transfer of the pool water, the convection heat transfer of the pool water surface, the heat conduction of the pool wall and the heat radiation process. For partial loss-of-water accidents, the evaporation/boiling heat transfer of the pool water is the main heat transfer mode. A total loss-of-coolant accident in an SFP is one of the application scenarios in which significant natural circulation flow occurs inside the spent fuel tank, which is an extremely severe accident. Since the spent fuel is exposed to the air, radiation heat transfer is inevitable. Therefore, natural convection and thermal radiation are the main heat transfer modes of a total loss-of-coolant accident. Lu et al. [70] established a model of an SFP and a plant at a scale of 1:8, and experimentally studied the natural circulation phenomenon in the event of a LOCA. Natural ventilation with ambient air can significantly slow down the temperature rise of FA, and spray can quickly reduce the temperature of FA. Hanisch et al. [71] studied the heat transfer characteristics of partially exposed FA using an ALADIN test bench (see Figure 11) and the results show that the cladding temperature increases with the exposure length. Josip et al. [72] evaluated the possibility and mitigation strategy of a LOCA. Partman et al. [73] studied the water level during a LOCA. In the initial stage, with the heating of the spent fuel, the water density decreases, the volume increases and the water level rises. When the temperature is higher than 70 °C, the mass flux of water evaporation increases with the increase in the water temperature and the water level drops. Tsao et al. [74] used 5 × 5 electric heating rods instead of spent fuel, and experimentally studied the influence of the bottom design of the fuel assembly storage rack on the cooling capacity of natural air circulation. Liu et al. [75,76] built a full-scale PWR spent fuel natural circulation test bench for total loss-of-water accidents, as shown in Figure 12, proposed a new flow resistance model suitable for low Re and established a RELAP5 model for the radiative heat transfer of spent fuel. They pointed that when the temperature difference between spent fuel and air is less than 150 °C, the natural air circulation flow rate is positively correlated with the temperature difference. When the temperature difference is greater than 150 °C, the natural air circulation flow rate will not change with the temperature difference. Oertel et al. [77] studied the accident process of a LOCA with partial spent fuel and pointed out that spent fuel with a high decay heat near the pool wall was beneficial to heat transfer. As the decay heat power around the spent fuel is the same, the horizontal direction of the spent fuel assembly is adiabatic. Therefore, the main cooling direction is along the axial direction [78].

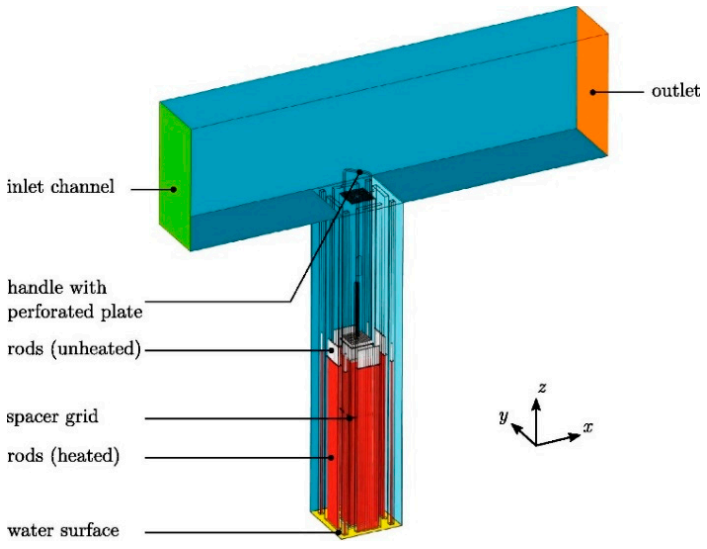

Figure 11. ALADIN test bench [71].

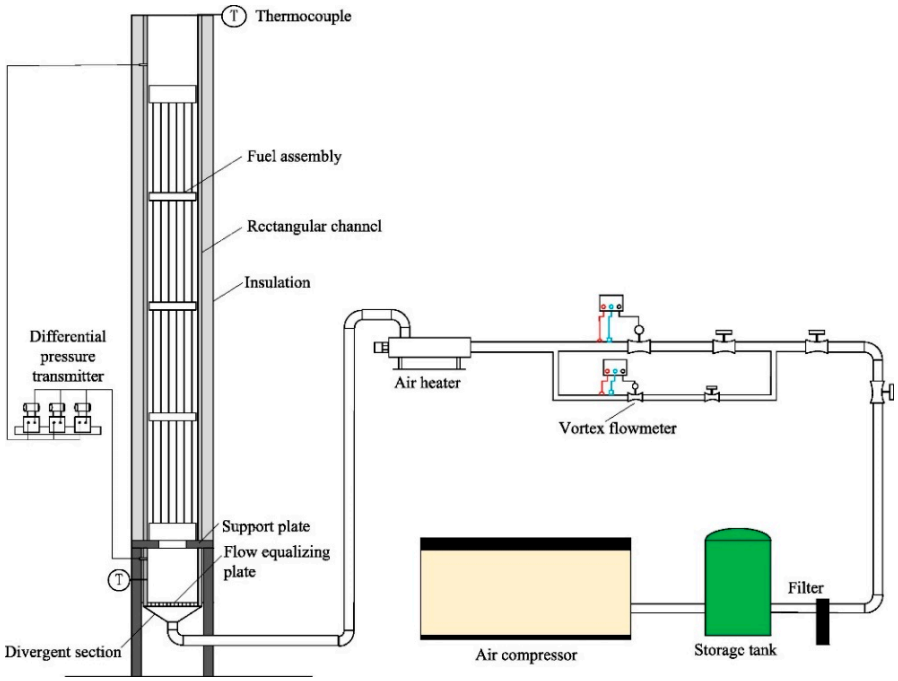

Figure 12. Schematic of a loss-of-water accident test bench [75].

Yu [79] established a PWR fuel bundle model, with each fuel bundle consisting of 264 fuel rods and 25 control rods, as shown in Figure 13. It is pointed out that increasing the gap size between fuel rods is beneficial for enhancing heat convection and radiation transfer. Mochizuki et al. [80] used RELAP5-3d code and manual calculation to study the water evaporation of an SFP during a power outage. Compared with the measured results, the RELAP5 code underestimated the collapsed water level. This shows that the void model under normal pressure should be modified to obtain a faster bubble rising speed. Zhang et al. [81] used RELAP5 and MELCOR to compare the LOCA process before fuel degradation, and the two codes have good consistency in the aspects of pool water temperature, water level drop and natural circulation response. The calculation differences in the temperature rise start time, peak cladding temperature time and oxidation threshold temperature time range from 5% to 15%. It can be concluded that the computational consistency between these two codes is guaranteed and that using code analysis is feasible.

Wu et al. [82] simulated the lost cooling process of the SFP of CPR1000 with MAAP5 code. For high-density storage racks, natural air circulation is not sufficient to cool the spent fuel. It is recommended that the space between adjacent components be expanded to improve the natural air circulation rate and to maintain the SFP cooling performance. Gauntt et al. [83] analyzed the LOCA of Fukushima unit-4 using TRACE code and predicted the boiling time, the water level drop process and the temperature rise of spent fuel. Carlos et al. [84] also used the TRACE program to analyze the thermal hydraulic characteristics of an SFP cooling accident. Liao et al. [85] analyzed accidents caused by SBO and FLB based on the ASTEC program. The results show that the accident process is relatively slow. When spent fuels are exposed and damaged, a large amount of hydrogen and fission products is released. Generally speaking, there are no mitigation measures to cope with this situation. Omidifard et al. [86] used MELCOR1.8.6 code to simulate the SFP of the VVER-1000/V446 nuclear reactor and pointed out that the SFP of the VVER-1000/V446 nuclear reactor might experience serious issues without mitigation measures in the event of a LOCA. Ahn et al. [7] used MELCOR to analyze the potential serious accidents that may occur in a PWR. Adorni et al. [87] evaluated the ignition process of fuel cladding in the event of a LOCA with three codes—ATHLET-CD, MELCOR and CFD—and pointed out that ATHLET-CD and MELCOR can capture the ignition time and maximum temperature with reasonable accuracy, while the CFD code has development potential in the future.

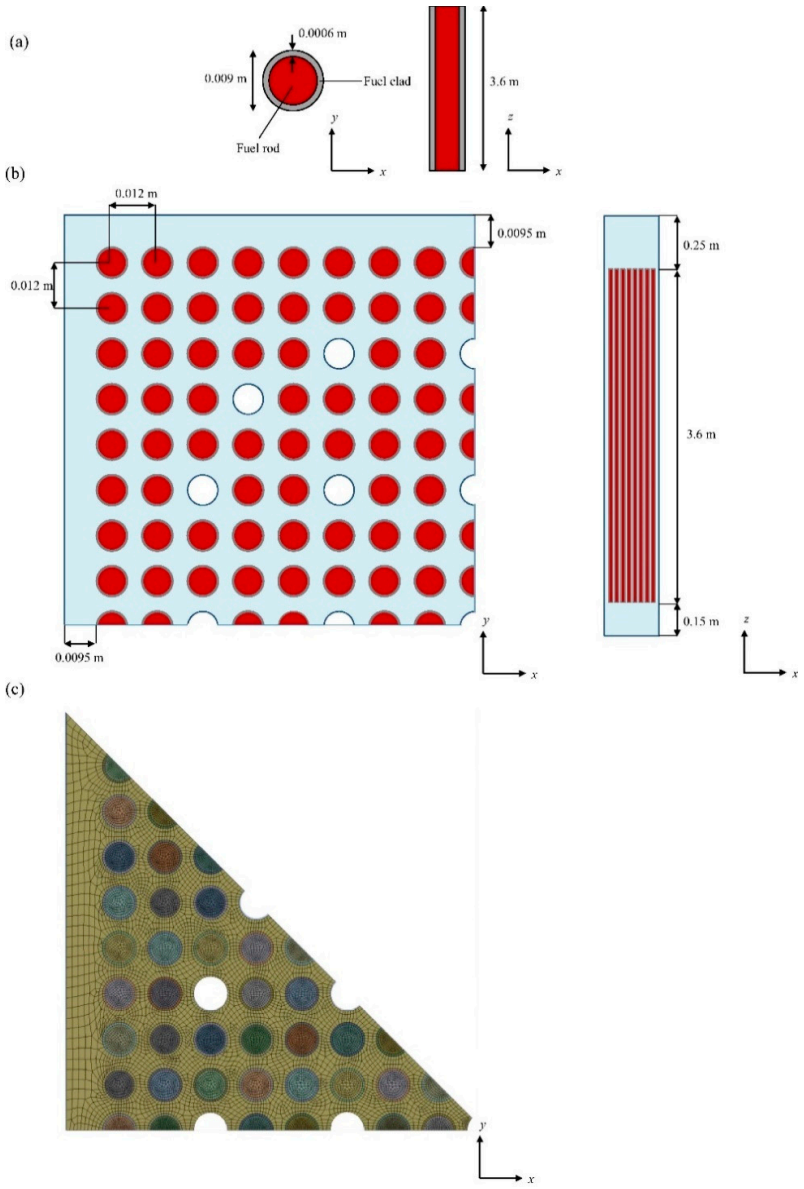

Figure 13. Schematic illustrating the fuel rod [79]. (**a**) fuel rod, (**b**)quartered fuel bundle (**c**) mesh pattern for one-eighth of the fuel bundle in the midplane.

Boyd [88] proposed to simplify the spent fuel and storage rack in a porous media model, and simulated the peak fuel temperature and flow patterns in the event of a LOCA using an equivalent thermal conductivity model. Huan et al. [89] also established a three-dimensional CFD model to simulate the thermal hydraulic characteristics of an SFP. When the cooling system fails, due to the rising temperature and the lowering of the water level, the spent fuel will be exposed and local boiling will occur. It is suggested that the spent fuel be placed on both sides of the pool for better heat exchange. Edward et al. [90] used Fluent to simulate the heat transfer characteristics of a 9 × 9 BWR fuel assembly in the event of a complete loss-of-coolant accident and proved the feasibility of CFD modeling. Chen et al. [91] set up a three-dimensional CFD model to simulate the temperature rising behavior of the 17 × 17 spent fuel assembly of Maanshan NPP in the event of a LOCA, as shown in Figure 14. The simulated average coolant temperature rising rate was 1.26 K/h. According to this temperature rising rate, it can be estimated that the maximum time required for the coolant to increase from the initial temperature of 317 K to the saturation temperature of 373 K is about 44 h during a LOCA.

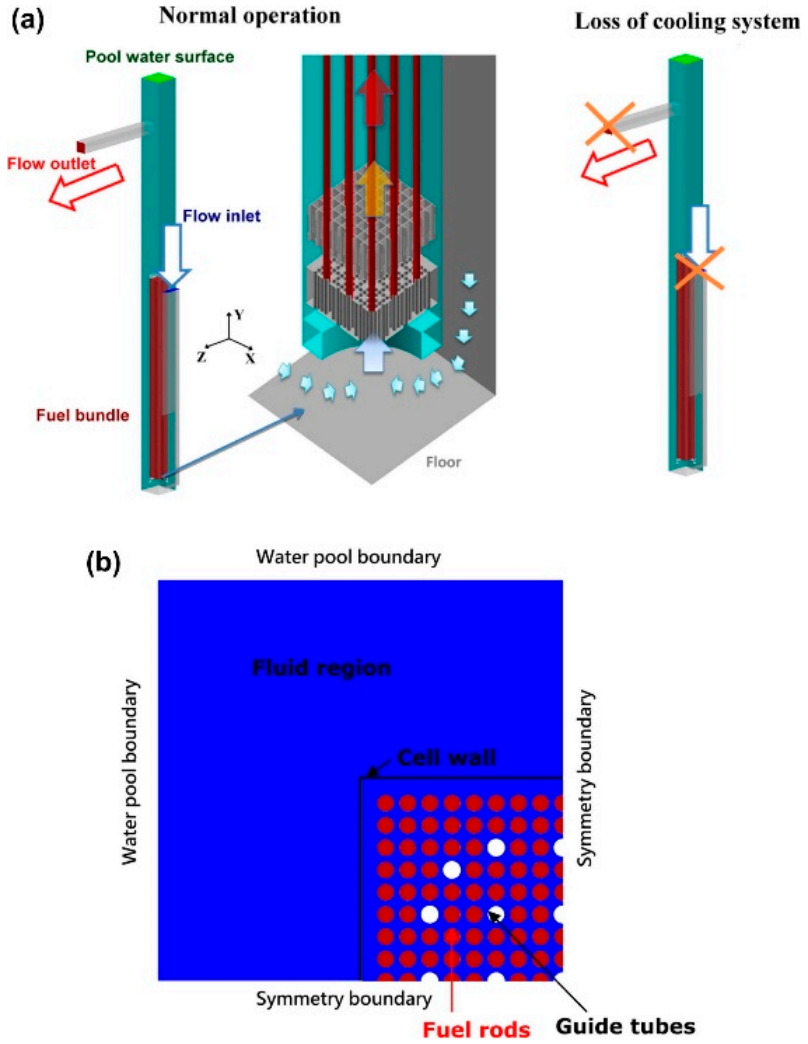

Figure 14. Schematic of simulation domain [91]. (**a**) 3D view (**b**) top view.

3.2. Development of Thermal Hydraulic Analysis Program

There are three ways to analyze the thermal hydraulic characteristics of an SFP: experimental, CFD and accident code program research. Due to the particularity of nuclear power equipment, the conditions for carrying out large-scale experiments are very harsh. Therefore, accident code program research and the CFD method are the main choices for studying the thermal hydraulic characteristics of nuclear energy equipment.

The safety accident analysis and additional storage requirements of SFPs are the driving forces for the development of thermal hydraulic analysis software. In the early stages, the software functions were generally singular and the model was simple. Renner et al. [92] developed a thermodynamic calculation program, SFPT, for SFPs. A one-dimensional model of the program was adopted, containing a calculation module for the flow path in the spent fuel assembly and the descending flow path between the storage grid and the pool wall. Gay et al. [93] improved the SFPT software and developed a three-dimensional transient SFP analysis code, GFLOW, in which a thermal radiation model was added to predict the temperature distribution. The calculation codes of SFPT and GFLOW are relatively simple, and the physical fluid parameters are constants, requiring users to input the hydraulic loss coefficient. Then, the SFUEL program—including heat conduction, convection, radiation and spent fuel cladding reaction models—was developed [94]. Nourbakhsh et al. [95] reported the analysis code SHARP, which can predict the temperature of FA during a LOCA. Rector [96] developed a three-dimensional analysis program, COBRA-SFS, based

on the finite volume subchannel simulation method, which clearly showed the heat flow distribution characteristics of an SFP. In recent years, with the development of safety analysis technology, MELCOR and RELAP have gradually been applied to the field of severe accident thermal hydraulic analysis. The MELCOR program is a serious accident analysis program developed by SANDIA [97]. It calculates all kinds of physical processes of serious accidents in a unified framework, and the calculation range includes the thermal hydraulic response in the reactor cooling system and containment, the heating, melting, collapse and repositioning of fuel assemblies, the cladding reaction process and other transient response processes. RELAP is a highly general accident analysis program developed by INEL, which can calculate the transient behavior of a reactor cooling system, and can also be used for various types of thermal hydraulic transient simulations of nuclear power and conventional systems.

MELCOR and RELAP5 can better predict the transient trend of SFP heat transfer performance. Compared with RELAP5, MELCOR is more simplified in terms of model processing, but both programs need to be improved with regard to the accuracy of their calculation models [81,98–101]. Moreover, TRACE [83,84], ASTEC [85,101,102], MAAP [99] and CFD [77,89–91] software have gradually become the tools of accident analysis for researchers.

4. Conclusions

Based on this review, it can be concluded that:

(1) With the rapid development of nuclear power technology, more and more FA is stored in the pool and the safety of SFP is increasingly important. Compared with existing SFP cooling systems, the safety of this system depends on the external energy supply system. If the energy supply system breaks down, it may cause a serious accident. Most NPPs increase the redundancy of their systems by adding cooling columns, equipment and various cold sources to ensure safety, but this also increases the construction costs of the system.

(2) PCSs for SFPs are only in the preliminary design stages, and the water loss time of the in Fukushima NPP is much longer than the 72 h preset of AP1000, meaning that the passive cooling capacity is limited. The existing research on the passive cooling systems of SFPs mainly focuses on separated heat pipes. The heat source temperature has a great influence on the heat transfer performance of PCSs, and the filling ratio of the loop is between 20% and 80%. Heat pipes should have good material compatibility, high latent heat, high level of safety, suitable working pressure and affordable price. Although the ammonia heat pipe has the strongest heat transfer capacity, it has potential safety hazards due to its explosive, toxic and poor material compatibility, so R134 a seems to be a more suitable choice. In the future, research on the heat transfer characteristics of working fluids such as methanol, ethanol, acetone and nanofluids should be carried out. The arrangement of the air-cooling tower is helpful to enhance the heat transfer capacity of PCSs.

(3) Most studies try to estimate the heat transfer performance of a single heat pipe module, lacking the overall study of the PCS, and only reveal the influence of a single parameter on the heat transfer of the PCS, without trying to integrate the parameters. As a result, a great deal of sensitivity analysis work remains to be carried out.

(4) Spent fuel with high decay power should be dispersed in an SFP. Reducing the ambient temperature and spraying have a significant effect on ensuring the safety of an SFP. After an accident, ventilation and spraying can be implemented to quickly cool down the pool.

(5) The RELAP and MELCOR programs have a good calculation consistency, and are widely used to calculate the thermal hydraulic characteristics and conduct accident analysis of SFPs. In the future, the programs should be optimized to improve their calculation accuracy and predict the accident progress.

(6) From a safety point of view, compared with a LOCA in the reactor core, the low attenuation heat and large amount of cooling water mixed with the spent fuel in an

SFP may slow down the accident process, but the large number of fuel assemblies stored in the SFP and the lack of containment may pose greater risks.

(7) The application of the PCS of the SFP in practice requires an overall experiment using a separated heat pipe cooling system, a performance analysis of the cooling system in the event of a LOCA and a reliability analysis of the cooling system and the layout of the spent fuel plant, as well as a seismic analysis.

Author Contributions: Conceptualization, C.X.; methodology, C.X. and S.T.; validation, Z.W. and X.C.; formal analysis, X.Z.; investigation, C.X.; writing—original draft preparation, C.X. and N.W.; writing—review and editing, Y.L. and S.T.; supervision, N.W.; project administration, N.W. All authors have read and agreed to the published version of the manuscript.

Funding: This research received no external funding.

Data Availability Statement: Not applicable.

Conflicts of Interest: The authors declare no conflict of interest.

References

1. Marco, C.; Paolo, C.; Zeynep, G.; Brianna, L.; Bertrand, M.; Mario, T.; Hal, T.; Aliki, V. *Climate Change and Nuclear Power 2022*; International Atomic Energy Agency: Vienna, Austria, 2022.
2. Azam, A.; Rafiq, M.; Shafique, M.; Zhang, H.; Yuan, J. Analyzing the effect of natural gas, nuclear energy and renewable energy on GDP and carbon emissions: A multi-variate panel data analysis. *Energy* **2019**, *219*, 119592. [CrossRef]
3. Bernard, L. *Statistical Review of World Energy 2021*; BP: London, UK, 2022.
4. Ewing, R. Nuclear Fuel Cycle: Environmental Impact. *MRS Bull.* **2008**, *33*, 338–340. [CrossRef]
5. Sanders, M.; Sanders, C. *Nuclear Waste Management Strategies-An International Perspective*; Elsevier Academic Press: London, UK, 2019. [CrossRef]
6. Vitkova, M.; Gorinov, I.; Dacheva, D. Safety criteria for wet and dry spent fuel storage. In Proceedings of the International Conference on WWER Fuel Performance, Modelling and Experimental Support, Albena, Bulgaria, 19–23 September 2005.
7. Ahn, K.I.; Shin, J.U.; Kim, W.T. Severe accident analysis of plant-specific spent fuel pool to support a SFP risk and accident management. *Ann. Nucl. Energy* **2016**, *89*, 70–83. [CrossRef]
8. Jin, H.S.; Kim, T.W. Severe accident issues raised by the Fukushima accident and improvements suggested. *Nucl. Eng. Technol.* **2014**, *46*, 207–216. [CrossRef]
9. Moamen, G.; Tawfic, A.F.; Chidiac, S.E. Spent nuclear fuel interim dry storage; Design requirements, most common methods, and evolution: A review. *Ann. Nucl. Energy* **2021**, *160*, 108408. [CrossRef]
10. Laura, R.P.; Soria, M. A Review of the Nuclear Fuel Cycle Strategies and the Spent Nuclear Fuel Management Technologies. *Energies* **2017**, *10*, 1235. [CrossRef]
11. Zhang, Y.J.; Huang, Z.R.; Zhao, F.Y. Mathematical modeling and evaluation of the safety culture for the operating nuclear power plants in China: Critical review and multi-criteria decision analysis. *Ann. Nucl. Energy* **2021**, *168*, 108871. [CrossRef]
12. Saegusa, T.; Wataru, M.; Shirai, K.; Takeda, H.; Namba, K. *Transport and Storage of Spent Nuclear Fuel-Safe and Secure Transport and Storage of Radioactive Materials*; Woodhead Publishing: Oxford, UK, 2015.
13. Hu, G.; Pfingsten, W. Data-driven machine learning for disposal of high-level nuclear waste: A review. *Ann. Nucl. Energy* **2023**, *180*, 109452. [CrossRef]
14. Surip, W.; Putraa, N.; Anhar, R.A. Design of passive residual heat removal systems and application of two-phase thermosyphons: A review. *Prog. Nucl. Energy* **2022**, *154*, 104473. [CrossRef]
15. Bevilacqua, A.; Carreton, J.; Guskov, A.; Hornebrant, T.; Jones, C. *Guidebook on Spent Fuel Storage*; International Atomic Energy Agency: Vienna, Austria, 1984.
16. Zhou, K.F.; Zheng, J.Y.; Feng, J.J. Analysis on mitigation measures of M310 Type NPP in SBO accident. *At. Energy Sci. Technol.* **2014**, *48*, 1464–1472. [CrossRef]
17. Liu, Z.; Liu, C.; Hongqiao, R. Research on Reverse-Heating for Test of Heat Exchanger of Spent Fuel Pool in EPR Units. *Nucl. Power Eng.* **2017**, *38*, 113–116. [CrossRef]
18. Cherubini, M.; Muellner, N.; D'Auria, F. Application of an optimized AM procedure following a SBO in a VVER-1000. *Nucl. Eng. Des.* **2008**, *238*, 74–80. [CrossRef]
19. Sutharshan, B.; Mutyala, M.; Vijuk, R.P. The AP1000TM Reactor: Passive Safety and Modular Design. *Energy Procedia* **2011**, *7*, 293–302. [CrossRef]
20. Schulz, T.L. Westinghouse AP1000 advanced passive plant. *Nucl. Eng. Des.* **2006**, *236*, 1547–1557. [CrossRef]
21. Xing, J.; Song, D.; Wu, Y. HPR1000: Advanced pressurized water reactor with active and passive safety. *Engineering* **2016**, *2*, 79–87. [CrossRef]
22. Li, J.; Li, X.M.; Yu, X.L. Design and Evaluation of Passive Containment Heat Removal System. *At. Energy Sci. Technol.* **2018**, *52*, 1021–1027. [CrossRef]

23. Aksan, N.; Choi, J.; Chung, Y.; Cleveland, J.; D'Auria, F. *Passive Safety Systems and Natural Circulation in Water Cooled Nuclear Power Plants*; International Atomic Energy Agency: Vienna, Austria, 2009.
24. Ye, C.; Zheng, M.G.; Han, X. Comparative Advantages of AP1000 Passive Safety System. *At. Energy Sci. Technol.* **2012**, *46*, 1221–1225. [CrossRef]
25. Jouhara, H.; Chauhan, A.; Nannou, T. Heat pipe based systems—Advances and applications. *Energy* **2017**, *128*, 729–754. [CrossRef]
26. Yin, X.; Hu, J.; Chi, X.Y. Experimental investigation of two-phase thermosyphon loop for passive containment cooling. *Appl. Therm. Eng.* **2021**, *184*, 116403. [CrossRef]
27. Wang, N.; Cui, Z.; Burger, J. Transient behaviors of loop heat pipes for alpha magnetic spectrometer cryocoolers. *Appl. Therm. Eng.* **2014**, *68*, 1–9. [CrossRef]
28. Fuchs, T. New Technical Concepts of Spent Fuel Pool-Cooling and Implementation. In Proceedings of the Annual Meeting on Nuclear Technology, Vienna, Austria, 29–30 September 2016.
29. Mochizuki, M.; Singh, R.; Nguyen, T. Heat pipe based passive emergency core cooling system for safe shutdown of nuclear power reactor. *Appl. Therm. Eng.* **2014**, *73*, 699–706. [CrossRef]
30. Mochizuki, M.; Singh, R.; Nguyen, T. An Emergency Core Cooling System (ECCS) for Nuclear Power Reactor Using Passive Loop Heat Pipe. *J. Jpn. Inst. Electron. Packag.* **2012**, *15*, 180–184. [CrossRef]
31. Kusuma, M.H.; Putra, N.; Antariksawan, A.R. Passive Cooling System in a nuclear spent fuel pool using a vertical straight wickless-heat pipe. *Int. J. Therm. Sci.* **2018**, *126*, 162–171. [CrossRef]
32. Kusuma, M.H.; Putra, N.; Ismarwanti, S. Simulation of wickless-heat pipe as passive cooling system in nuclear spent fuel pool using RELAP5/MOD3.2. *Int. J. Adv. Sci. Eng. Inf. Technol.* **2017**, *7*, 836–842. [CrossRef]
33. Kusuma, M.H.; Putra, N.; Antariksawan, A.R. Investigation of the Thermal Performance of a Vertical Two-Phase Closed Thermosyphon as a Passive Cooling System for a Nuclear Reactor Spent Fuel Storage Pool. *Nucl. Eng. Technol.* **2017**, *49*, 476–483. [CrossRef]
34. Choi, J.; Lim, C.; Kim, H. Fork-end heat pipe for passive air cooling of spent nuclear fuel pool. *Nucl. Eng. Des.* **2021**, *374*, 111081. [CrossRef]
35. Lim, C.; Choi, J.; Kim, H. Experimental Investigation of the Heat Transfer Characteristics and Operation Limits of a Fork-Type Heat Pipe for Passive Cooling of a Spent Fuel Pool. *Energies* **2021**, *14*, 7862. [CrossRef]
36. Ye, C.; Wang, M.; Qiu, Z. The Comparative Advantages of CAP1400 Nuclear Power Plant Passive Safety System. In Proceedings of the 5th International Conference on Nuclear Engineering, Shanghai, China, 2–6 July 2017.
37. Ye, C.; Zheng, M.G.; Wang, M.L. The design and simulation of a new spent fuel pool passive cooling system. *Ann. Nucl. Energy* **2013**, *58*, 124–131. [CrossRef]
38. Xiong, Z.Q.; Wang, M.L.; Gu, H.Y. Experimental study on heat pipe heat removal capacity for passive cooling of spent fuel pool. *Ann. Nucl. Energy* **2015**, *83*, 258–263. [CrossRef]
39. Xiong, Z.Q.; Ye, C.; Wang, M.L. Experimental study on the sub-atmospheric loop heat pipe PCS for spent fuel pool. *Prog. Nucl. Energy* **2015**, *79*, 40–47. [CrossRef]
40. Xiong, Z.Q.; Gu, H.Y.; Wang, M.L. The thermal performance of a loop-type heat pipe for passively removing residual heat from spent fuel pool. *Ann. Nucl. Energy* **2014**, *280*, 262–268. [CrossRef]
41. Zheng, H.; Ma, W.M. Performance of a passive cooling system for spent fuel pool using two- phase thermosiphon evaluated by RELAP5/MELCOR coupling analysis. *Ann. Nucl. Energy* **2019**, *128*, 330–340. [CrossRef]
42. Li, G.; Wang, H.T.; Zhang, G.L. Thermal-hydraulic design and transient analysis of PCS for CPR1000 spent fuel storage pool. *Nucl. Sci. Technol.* **2016**, *27*, 8. [CrossRef]
43. Kuang, Y.W.; Yi, C.C.; Wang, W. Heat transfer performance analysis of a large-scale separate heat pipe with a built-in tube. *Appl. Therm. Eng.* **2020**, *167*, 114726. [CrossRef]
44. Wu, Y.X.; Cheng, J.J.; Zhu, H. Experimental study on heat transfer characteristics of separated heat pipe with compact structure for spent fuel pool. *Ann. Nucl. Energy* **2023**, *181*, 109580. [CrossRef]
45. Luo, Y.; Wang, W.; Hu, Y.L. Experimental Study on Heat Transfer Characteristics of Separated Heat Pipe Loop with Multi-parallel Branches. *J. Refrig.* **2019**, *40*, 32–36.
46. Han, F.; Kuang, Y.W.; Ye, C. Investigation on thermal-hydraulic characteristics of the spent fuel pool with a complete passive cooling system. *Ann. Nucl. Energy* **2022**, *177*, 109326. [CrossRef]
47. Kuang, Y.W.; Yi, C.C.; Wang, W. Modeling and simulation of large-scale separated heat pipe with low heat flux for spent fuel pool cooling. *Appl. Therm. Eng.* **2019**, *147*, 747–755. [CrossRef]
48. Kuang, Y.; Yang, Q.; Wang, W. Thermal analysis of a heat pipe assisted passive cooling system for spent fuel pools. *Int. J. Refrig.* **2022**, *135*, 174–188. [CrossRef]
49. Kuang, Y.; Wang, W. Modeling and numerical investigation on effects of filling ratio in a large separate heat pipe loop. *Int. J. Energy Res.* **2022**, *46*, 415–432. [CrossRef]
50. Fu, W.; Li, X.W.; Wu, X.X. Investigation of a long term passive cooling system using two-phase thermosyphon loops for the nuclear reactor spent fuel pool. *Ann. Nucl. Energy* **2015**, *85*, 346–356. [CrossRef]
51. Kusuma, M.H.; Putra, N.; Rosidi, A. Investigation on the Performance of a Wickless-Heat Pipe Using Graphene Nanofluid for Passive Cooling System. *At. Indones.* **2019**, *45*, 173–182. [CrossRef]

52. Kundu, A.; Kumar, R.; Gupta, A. Comparative experimental study on flow boiling heat transfer characteristics of pure and mixed refrigerants. *Int. J. Refrig.* **2014**, *45*, 136–147. [CrossRef]
53. Enoki, K.; Ono, M.; Okawa, T. Water flow boiling heat transfer in vertical minichannel. *Exp. Therm. Fluid Sci.* **2020**, *117*, 110147. [CrossRef]
54. Kuang, Y.W.; Wen, W.; Rui, Z. Simulation of boiling flow in evaporator of separate type heat pipe with low heat flux. *Ann. Nucl. Energy* **2015**, *75*, 158–167. [CrossRef]
55. Lima, L.; Mangiavacchi, N.; Ferrari, L. Stability analysis of passive cooling systems for nuclear spent fuel pool. *J. Braz. Soc. Mech. Sci. Eng.* **2017**, *39*, 1019–1031. [CrossRef]
56. Yang, K.M.; Wang, N.H.; Jiang, C.H. Experimental Research and Simulation in a Thermosyphon. *Adv. Mater. Res.* **2012**, *580*, 441–444. [CrossRef]
57. Yang, K.M.; Wang, N.H.; Jiang, C.H. An Investigation of the Thermal Performance of a Novel Axial Grooved Heat Pipe. *Adv. Mater. Res.* **2012**, *580*, 223–226. [CrossRef]
58. Lai, K.; Wang, W.; Yi, C.C. The study of passive cooling system assisted with separate heat pipe for decay heat removal in spent fuel pool. *Ann. Nucl. Energy* **2018**, *111*, 523–535. [CrossRef]
59. Unger, S.; Krepper, E.; Hampel, U. Numerical analysis of heat exchanger designs for passive spent fuel pool cooling to ambient air. *Nucl. Eng. Des.* **2018**, *333*, 224–234. [CrossRef]
60. Unger, S.; Krepper, E.; Beyer, M. Numerical optimization of a finned tube bundle heat exchanger arrangement for passive spent fuel pool cooling to ambient air. *Nucl. Eng. Des.* **2020**, *361*, 110549. [CrossRef]
61. Unger, S.; Arlit, M.; Beyer, M. Experimental study on the advective heat flux of a heat exchanger for passive cooling of spent fuel pools by temperature anemometry grid sensor. *Nucl. Eng. Des.* **2021**, *379*, 111237. [CrossRef]
62. Rigby, A.; Lindley, B.; Cullen, J. An exergy based assessment of the efficiency of nuclear fuel cycles. *Energy* **2023**, *264*, 126160. [CrossRef]
63. Nuclear Energy Agency. *Status Report on Spent Fuel Pools under Loss-of-Cooling and Loss-of-Coolant Accident Conditions*; OECD Publishing: Paris, France, 2015.
64. Shi, B.G. Spent fuel natural circulation cooling analysis of chashma nuclear power plant. *Nucl. Power Eng.* **1999**, *20*, 413–416.
65. Benjamin, A.S.; Mccloskey, D.J. Spent Fuel Heatup Following Loss of Water during Storage. *Nucl. Technol.* **1980**, *49*, 274–294. [CrossRef]
66. Jo, J.; Rose, P.; Unwin, S.; Sailor, V.; Perkins, K.; Tingle, A. *Value/Impact Analyses of Accident Preventive and Mitigative Options for Spent Fuel Pools*; Nuclear Regulatory Commission: Rockville, MD, USA, 1989.
67. Throm, E. *Regulatory Analysis for the Resolution of Generic Issue 82 "Beyond Design Basis Accidents in Spent Fuel Pools"*; Nuclear Regulatory Commission: Rockville, MD, USA, 1989.
68. Timothy, E.; George, H. *Technical Study of Spent Fuel Pool Accident Risk at Decommissioning Nuclear Power Plants*; Nuclear Regulatory Commission: Rockville, MD, USA, 2001.
69. Siu, N.; Khericha, S.; Conroy, S.; Beck, S.; Blackman, H. *Loss of Spent Fuel Pool Cooling PRA: Model and Results*; Nuclear Regulatory Commission: Rockville, MD, USA, 1996.
70. Lu, Y.Z.; Yun, X.Y.; Zhang, H.Y. Experimental Research of Air Natural Circulation and Hydrogen Distribution in Fuel Building after Loss of Coolant Accident. *At. Energy Sci. Technol.* **2020**, *54*, 916–922. [CrossRef]
71. Hanisch, T.; Zedler, P.; Hurtado, A. Numerical and experimental analysis of flow and heat transfer in a fuel assembly mock-up with transverse flow above the rods. *Int. J. Heat Fluid Flow* **2021**, *89*, 108809. [CrossRef]
72. Josip, D.; Davor, G. Analysis of Spent Fuel Pool Loss of Coolant Inventory Accident Progression. *J. Energy* **2017**, *66*, 1–9.
73. Partmann, C.; Schuster, C.; Hurtado, A. Experimental investigation of the thermal hydraulics of a spent fuel pool under loss of active heat removal conditions. *Nucl. Eng. Des.* **2018**, *330*, 480–487. [CrossRef]
74. Tsao, P.; Hsieh, K.; Lee, D.; Kim, C.; Tseng, Y.; Hung, T. Investigation of passive air cooling capacity for spent fuel pool. In Proceedings of the World Congress on Advances in Nano, Biomechanics, Robotics, and Energy Research 2013, Seoul, Republic of Korea, 25–28 August 2017.
75. Liu, M.L.; Wang, L.; Ni, S. Experimental investigation on pressure drop of a PWR fuel assembly under low Re conditions. *Ann. Nucl. Energy* **2022**, *167*, 108768. [CrossRef]
76. Liu, M.L.; Ni, S.; Wang, X. Experimental study on the natural circulation behavior of a full-scale PWR fuel assembly. *Ann. Nucl. Energy* **2022**, *174*, 109172. [CrossRef]
77. Oertel, R.; Hanisch, T.; Krepper, E. Two-scale CFD analysis of a spent fuel pool involving partially uncovered fuel storage racks. *Nucl. Eng. Des.* **2019**, *341*, 432–450. [CrossRef]
78. Nuclear Energy Agency. *Nuclear Energy Agency Committee on the Safety of Nuclear Installations*; OECD Publishing: Paris, France, 2015.
79. Yu, C.L. Numerical study on hydrodynamic and thermal characteristics of spent fuel pool. *Ann. Nucl. Energy* **2018**, *119*, 139–147. [CrossRef]
80. Mochizuki, H. Evaluation of spent fuel pool temperature and water level during SBO. *Ann. Nucl. Energy* **2017**, *109*, 548–556. [CrossRef]
81. Zhang, Z.W.; Du, Y.; Liang, K.S. Advanced modeling techniques of a spent fuel pool with both RELAP5 and MELCOR and associated accident analysis. *Ann. Nucl. Energy* **2017**, *110*, 160–170. [CrossRef]

82. Wu, X.; Wei, L.; Zhang, Y. Analysis of accidental loss of pool coolant due to leakage in a PWR SFP. *Ann. Nucl. Energy* **2015**, *77*, 65–73. [CrossRef]
83. Gauntt, R.; Donald, K. *Fukushima Daiichi Accident Study*; Sandia National Laboratories: Albuquerque, NM, USA, 2012.
84. Carlos, S.; Martorell, S. Use of TRACE best estimate code to analyze spent fuel storage pools safety. *Prog. Nucl. Energy* **2014**, *77*, 224–238. [CrossRef]
85. Liao, F.Y.; Chen, W.H.; Guo, C. Study on Severe Accident Occurred in Spent Fuel Pool Based on ASTEC Code. *Nucl. Sci. Eng.* **2022**, *1*, 199–206.
86. Omidifard, P.; Pirouzmand, A.; Hadad, K. Analysis of loss of cooling and loss of coolant severe accident scenarios in VVER-1000/V446 spent fuel pool. *Ann. Nucl. Energy* **2020**, *138*, 107205. [CrossRef]
87. Adorni, M.; Herranz, L.E.; Hollands, T. OECD/NEA Sandia Fuel Project phase I: Benchmark of the ignition testing. *Nucl. Eng. Des.* **2016**, *307*, 418–430. [CrossRef]
88. Boyd, C. *Predictions of Spent Fuel Heatup after a Complete Loss of Spent Fuel Pool Coolant*; Nuclear Regulatory Commission: Rockville, MD, USA, 2000.
89. Hung, T.C.; Vijay, K.; Pei, B.S. The development of a three-dimensional transient CFD model for predicting cooling ability of spent fuel pools. *Appl. Therm. Eng.* **2013**, *50*, 496–504. [CrossRef]
90. Edward, J. *Development and Assessment of CFD Models Including a Supplemental Program Code for Analyzing Buoyancy-Driven Flows through BWR Fuel Assemblies in SFP Complete LOCA Scenarios*; The University of Texas at Austin: Austin, TX, USA, 2012. Available online: http://hdl.handle.net/2152/ETD-UT-2012-12-6836 (accessed on 16 April 2023).
91. Chen, S.R.; Lin, W.C.; Ferng, Y.M. CFD simulating the transient thermal–hydraulic characteristics in a 17 × 17 bundle for a spent fuel pool under the loss of external cooling system accident. *Ann. Nucl. Energy* **2014**, *73*, 241–249. [CrossRef]
92. Renner, H. SFPT-4 Computer Program for Multi-Channel Analysis of Spent Fuel Pool Natural Circulation. NUS-TM-285. 1976.
93. Gay, R.R. Spent Nuclear Fuel Storage Pool Thermal Hydraulic Analysis. *Prog. Nucl. Energy* **1984**, *14*, 199–255. [CrossRef]
94. Stalker, K.T.; Benjamin, A.S. Experimental Studies of Rapidly Oxidizing Zircaloy Cladding Bundles in Air. *Trans. Am. Nucl. Soc.* **1983**, *45*, 134–135.
95. Nourbakhsh, H.; Miao, G.; Cheng, Z. *Analysis of Spent Fuel Heatup Following Loss of Water in a Spent Fuel Pool: A Users' Manual for the Computer Code SHARP*; Nuclear Regulatory Commission: Rockville, MD, USA, 2002.
96. Michener, T.E.; Rector, D.R.; Cute, J. COBRA-SFS Thermal-Hydraulic Analysis Code for Spent-Fuel Storage and Transportation Casks: Models and Methods. *Nucl. Technol. A J. Am. Nucl. Soc.* **2017**, *199*, 330–349. [CrossRef]
97. Gauntt, R.; Cole, R.; Erickson, C.; Rodriquez, S. *MELCOR Computer Code Manuals Version 1.8.5*; Sandia National Laboratories: Albuquerque, NM, USA, 2000.
98. Kaliatka, A.; Ognerubov, V.; Vileiniskis, V. Analysis of the processes in spent fuel pools of Ignalina NPP in case of loss of heat removal. *Nucl. Eng. Des.* **2010**, *240*, 1073–1082. [CrossRef]
99. Vierow, K.; Liao, Y.; Johnson, J. Severe accident analysis of a PWR station blackout with the MELCOR, MAAP4 and SCDAP/RELAP5 codes. *Nucl. Eng. Des.* **2004**, *234*, 129–145. [CrossRef]
100. Nim, S.; Liu, M.L.; Gu, H.Y. Modeling and validation of RELAP5 for natural circulation flow in a single PWR fuel assembly. *Ann. Nucl. Energy* **2021**, *151*, 107940. [CrossRef]
101. Maccari, P.; Mascari, F.; Ederli, S.; Manservisi, S. SBO analysis of a generic PWR-900 with ASTEC and MELCOR codes. *J. Phys. Conf. Ser.* **2021**, *1868*, 012019. [CrossRef]
102. Ammirabile, L.; Bujan, A.; Sangiorgi, M. PWR Medium Break LOCA source term analysis using ASTEC code. *Prog. Nucl. Energy* **2015**, *81*, 30–42. [CrossRef]